Materials Advances

ROYAL SOCIETY OF CHEMISTRY

PAPER

View Article Online
View Journal | View Issue

Open Access Article. Published on 18 October 2021. Downloaded on 12/9/2025 7:48:21 AM.
This article is licensed under a Creative Commons Attribution-NonCommercial 3.0 Unported Licence.

Check for updates

Cite this: *Mater. Adv.*, 2022, 3, 312

Amphiphilic γ-cyclodextrin–fullerene complexes with photodynamic activity†

Koji Miki,[a]* Zi Dan Zhang,[a] Kaho Kaneko,[a] Yui Kakiuchi,[a] Kentaro Kojima,[a] Akane Enomoto,[a] Masahiro Oe,[a] Kohei Nogita,[a] Yasujiro Murata,[b] Hiroshi Harada[c] and Kouichi Ohe[a]*

Received 20th August 2021,
Accepted 17th October 2021

DOI: 10.1039/d1ma00743b

rsc.li/materials-advances

Amphiphilic γ-cyclodextrin–fullerene 2 : 1 complexes (C_LFC_H complexes) were prepared by high-speed vibration milling of lipophilic tail-grafted γ-cyclodextrin (γ-CD), hydrophilic tail-grafted γ-CD and fullerene C_{60}. The transamidation of γ-CD–fullerene complexes having two amino groups with lipophilic and hydrophilic activated esters also afforded amphiphilic C_LFC_H complexes. Self-assemblies consisting of amphiphilic C_LFC_H complexes efficiently generated singlet oxygen under photoirradiation. Under visible light irradiation conditions, C_LFC_H complexes bearing a vitamin E moiety as a lipophilic tail showed high photodynamic activity toward cancer cells.

Introduction

Photodynamic therapy (PDT) is one of the most promising and minimally invasive cancer therapies.[1] Photosensitizers which efficiently generate cytotoxic reactive oxygen species (ROS), such as singlet oxygen ($^1O_2$) and superoxide radical anions ($O_2^{\bullet-}$), under light irradiation are suitable as PDT agents.[1,2] Fullerenes have been extensively investigated as PDT agents, because the quantum yield of ROS generation from excited fullerenes is very high.[3] With the goal of practical use of fullerenes as a PDT agent, hydrophilic substituent-grafted fullerenes and water-soluble fullerene-containing nanocarriers have been explored.[3,4] Although functionalized fullerenes having hydrophilic substituents show low IC_{50} values, they cannot actively accumulate in a tumour site. For the passive accumulation[5] of fullerene-based PDT agents in a tumour site, the preparation of fullerene-containing nanocarriers with photodynamic activity has become a research topic of growing interest.[4] Ikeda and co-workers have recently reported the synthesis of fullerene-containing liposomes, in which the ROS was efficiently generated from fullerenes localized in the lipophilic segment of the lipid bilayer.[4a,6] However, the PDT properties of nanoparticles consisting of fullerene-containing amphiphiles have been less investigated.

γ-Cyclodextrin (γ-CD) is a macrocyclic oligosaccharide that can include fullerene (C_{60}) in its lipophilic cavity leading to a water-soluble complex, the γ-CD–fullerene–γ-CD (CFC) complex, with a bicapped structure (Fig. 1a).[7] The synthesis and application of CFC containing functionalized γ-CD derivatives have been barely investigated probably because of their low accessibility.[8] We assumed that amphiphilic CFCs consisting of γ-CDs with lipophilic and hydrophilic tails can form PDT-active self-assemblies in water (Fig. 1b). To develop unsymmetric lipophilic γ-CD–fullerene–hydrophilic γ-CD (C_LFC_H) complexes, we envisioned two approaches, mechanochemical high-speed-vibration milling (HSVM, Method A in Fig. 2)[9] and

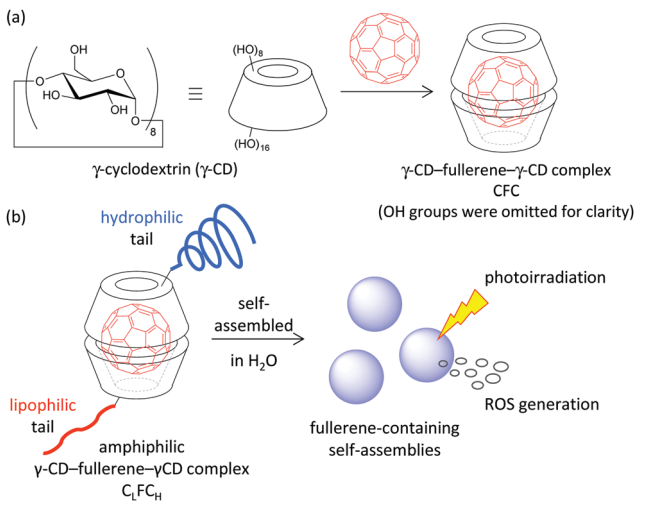

Fig. 1 (a) γ-CD–fullerene–γ-CD complex CFC. (b) Amphiphilic γ-CD–fullerene–γ-CD complex C_LFC_H (this study).

[a] Department of Energy and Hydrocarbon Chemistry, Graduate School of Engineering, Kyoto University, Katsura, Nishikyo-ku, Kyoto 615-8510, Japan. E-mail: kojimiki@scl.kyoto-u.ac.jp, ohe@scl.kyoto-u.ac.jp
[b] Institute of Chemical Research, Kyoto University, Uji, Kyoto 611-0011, Japan
[c] Laboratory of Cancer Cell Biology, Graduate School of Biostudies, Kyoto University, Yoshida Konoe-cho, Sakyo-ku, Kyoto 606-8501, Japan

† Electronic Supplementary Information (ESI) available. See DOI: 10.1039/d1ma00743b

© 2022 The Author(s). Published by the Royal Society of Chemistry

Open Access Article. Published on 18 October 2021. Downloaded on 12/9/2025 7:48:21 AM.
This article is licensed under a Creative Commons Attribution-NonCommercial 3.0 Unported Licence.

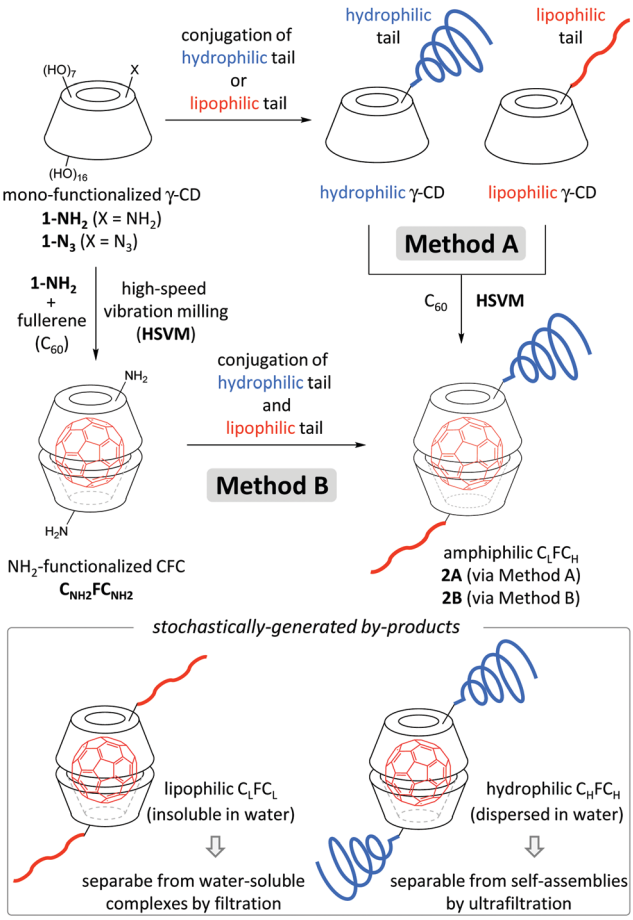

Fig. 2 Preparation of amphiphilic C_LFC_H through HSVM of C_{60} with lipophilic and hydrophilic γ-CDs [Method A] and functionalization of amino-functionalized CFC $\mathbf{C_{NH2}FC_{NH2}}$ [Method B].

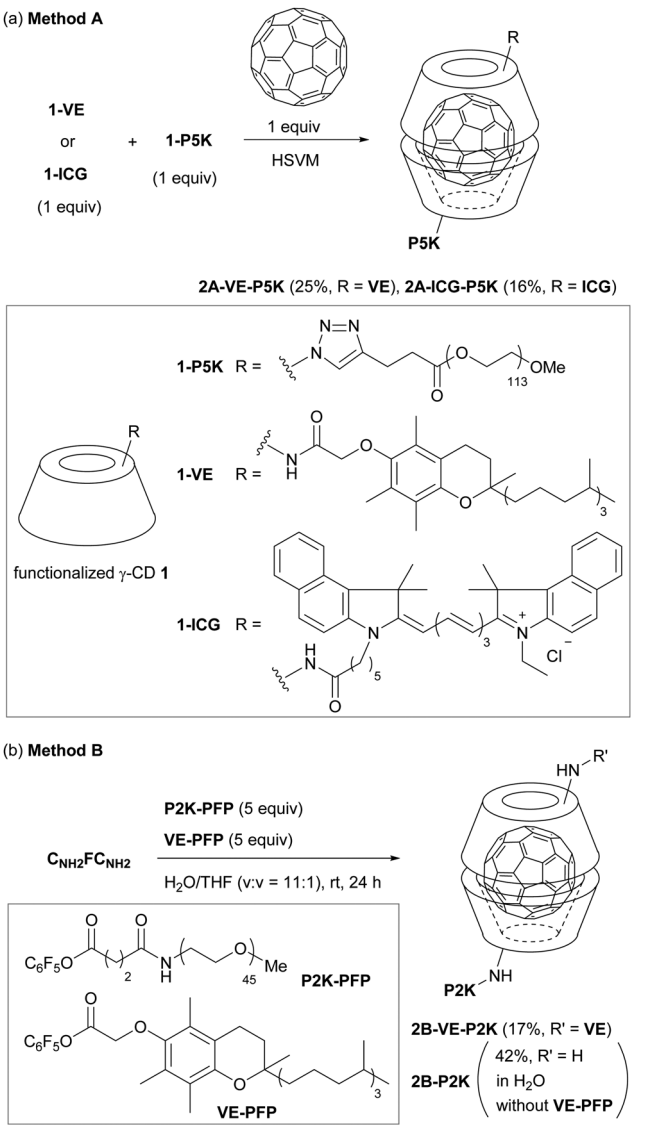

Fig. 3 Synthesis of (a) C_LFC_H **2A** through HSVM with mono-functionalized γ-CD derivatives **1** [Method A] and (b) C_LFC_H **2B** through functionalization of $\mathbf{C_{NH2}FC_{NH2}}$ [Method B]. PFP: pentafluorophenoxy group.

post-complexation functionalization (Method B in Fig. 2). Komatsu, Murata and co-workers reported that the HSVM technique affords symmetrically functionalized CFC complexes efficiently.[10] Recently, Hoogenboom and co-workers reported the HSVM-assisted preparation of water-soluble self-assemblies consisting of functionalized γ-CD and C_{60}.[11] However, there are no reports of unsymmetrically functionalized CFC complexes synthesized through HSVM of two γ-CD derivatives and C_{60}. In the course of our study, we found that amphiphilic unsymmetric C_LFC_H complexes can be obtained by HSVM and size-selective filtration. We also found that the conjugation of lipophilic and hydrophilic substituents with the preformed CFC affords amphiphilic unsymmetric C_LFC_H complexes. We here report the preparation of self-assemblies of amphiphilic C_LFC_H complexes and their photoinduced cytotoxicity.

Results and discussion

Functionalized γ-CD derivatives **1** (Fig. 3) were obtained from accessible 6-monoazido-6-deoxy-γ-cyclodextrin $\mathbf{1\text{-}N_3}$[12] (see the ESI†). The γ-CD derivative **1-P5K** having poly(ethylene glycol) (PEG, average molecular weights: 5000) as a hydrophilic tail was synthesized by the copper-mediated [3+2] cyclization reaction. The γ-CD derivatives **1-VE** and **1-ICG** having a lipophilic tocopherol (vitamin E; VE) and near-infrared indocyanine green (ICG)[13] dye were synthesized by transamidation of 6-mono-amino-6-deoxy-γ-cyclodextrin $\mathbf{1\text{-}NH_2}$.[12]

We examined HSVM of C_{60} with **1-P5K** and lipophilic tail-grafted γ-CD derivatives by an in-house built vibrating machine at 3500 rotations per minute (rpm) or a commercially available machine at 1800 rpm (Fig. 3a, Method A). Under HSVM conditions for 30 min, amphiphilic C_LFC_H complexes **2A** were produced. C_LFC_H complexes **2A** could be purified from an aqueous suspension of the crude product using sequential filtration.[14] Water-insoluble unreacted C_{60} and stochastically generated symmetric C_LFC_L complexes were removed by filtration using a syringe filter (pore size: 0.45 μm). Amphiphilic C_LFC_H

Open Access Article. Published on 18 October 2021. Downloaded on 12/9/2025 7:48:21 AM.
This article is licensed under a Creative Commons Attribution-NonCommercial 3.0 Unported Licence.

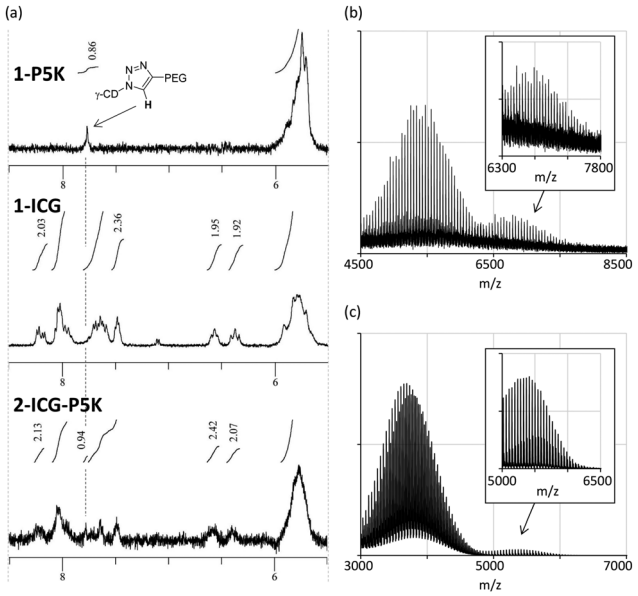

Fig. 4 (a) ^{1}H NMR spectra (d_6-DMSO, 25 °C, 400 MHz) of **1-P5K**, **1-ICG** and **2A-ICG-P5K**. MALDI-TOF mass spectra of (b) **2A-ICG-P5K** and (c) **2B-VE-P2K**.

complexes **2A**, which form nanometer-sized self-assemblies in water, could be separated from unreacted γ-CDs and water-soluble symmetric C_HFC_H complexes using ultrafiltration (MWCO: 50 K) as a size-specific separation method. It was confirmed that C_LFC_H complexes **2A** were composed of γ-CDs having lipophilic and hydrophilic tails in a ratio of *ca.* 1 : 1 in ^{1}H NMR measurement (Fig. 4a and Fig. S1 in the ESI†). In the MALDI-TOF mass spectrum of C_LFC_H complex **2A-ICG-P5K**, the parent signal was detected together with lipophilic and hydrophilic tail-grafted γ-CDs (Fig. 4b and Fig. S2 in the ESI†). In the UV-vis absorption spectra of aqueous solutions of **2A** in H_2O, a sharp signal at 330–340 nm and a broad signal at 400–700 nm attributed to C_{60} were observed (Fig. 5). Broadened signals at around 450 nm point out that C_LFC_H complexes **2A** contain non-capsulated C_{60} like γ-CD–C_{60} aggregates.[15] HSVM of C_{60} with excess amounts of **1-P5K**, followed by sequential filtration, afforded a small amount of water-soluble C_{60}-containing aggregates. The results from this control experiment indicate that the contamination of the γ-CD–C_{60} aggregate is not avoidable in Method A. Although the contamination was not negligible, it was estimated that molar extinction coefficients (at 332 nm) of **2A-VE-P5K** and **2A-ICG-P5K** in H_2O are 2.9×10^4 and 3.2×10^4 M^{-1} cm^{-1}, respectively. These extinction coefficient values are similar to the reported values ($1.2–4.3 \times 10^4$ M^{-1} cm^{-1}) of CFC complexes and C_{60}-containing liposomes.[4a,6,7b] In the case of **2A-ICG-P5K**, the broad absorption signal of an ICG tail was detected in the near-infrared region. This suggests that lipophilic ICG moieties interact with each other and form stacked aggregates in a lipophilic core.[16]

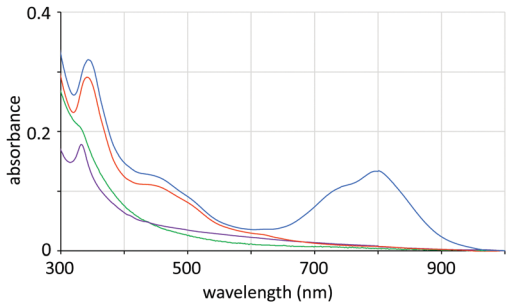

Fig. 5 UV-vis absorption spectra of an aqueous solution of **2A-VE-P5K** (red), **2A-ICG-P5K** (blue), **2B-VE-P2K** (green) and **2B-P2K** (purple). Concentration: 1.0×10^{-5} M.

To avoid the contamination of non-capsulated C_{60}, we next examined the functionalization of preformed CFC complex $\mathbf{C_{NH2}FC_{NH2}}$ (Fig. 3, Method B). Among several activated esters, we found that pentafluorophenyl esters **VE-PFP** and **P2K-PFP** bearing VE and P2K (PEG, average molecular weights: 2000) are suitable for the functionalization of $\mathbf{C_{NH2}FC_{NH2}}$. In H_2O/THF, amphiphilic C_LFC_H complex **2B-VE-P2K** could be synthesized from $\mathbf{C_{NH2}FC_{NH2}}$, **P2K-PFP** and **VE-PFP** in a moderate yield. The parent signals of **2B-VE-P2K** could be detected by MALDI-TOF mass spectroscopy (Fig. 4c). Under the identical conditions, the treatment of the activated ester bearing P5K moiety did not afford amphiphilic C_LFC_H complexes, probably because of low reactivity at the long polymer chains. The reaction of $\mathbf{C_{NH2}FC_{NH2}}$ with **P2K-PFP** afforded PEG-grafted CFC **2B-P2K** in moderate yield (Fig. S4 in the ESI†). In UV-vis absorption spectra of **2B**, the shoulder signal around 450 nm was not observed (Fig. 5). The molar extinction coefficients of **2B-VE-P2K** (2.1×10^4 M^{-1} cm^{-1}) and **2B-P2K** (1.8×10^4 M^{-1} cm^{-1}) are slightly lower than those of **2A**.

The hydrodynamic diameters of self-assemblies of C_LFC_H complexes determined by dynamic light scattering were 107 ± 28 (**2A-VE-P5K**), 87 ± 24 (**2A-ICG-P5K**), 194 ± 44 (**2B-VE-P2K**), and 322 ± 54 nm (**2B-P2K**), respectively (Fig. S6 in the ESI†). The diameters of self-assemblies in water and phosphate buffered saline (pH 7.4) were not changed for 10 days. The absorbance of self-assemblies was not decreased under visible light and/or under an oxygen atmosphere for several days.[17] This indicates that self-assemblies are stable enough to be handled in both solid and solution states. The particle morphology of CFCs was explored by transmission electron microscopy (TEM). In light of TEM images, spherical self-assemblies of **2A-VE-P5K**, **2A-ICG-P5K**, and **2B-VE-P2K** with average diameters (D_a) of 100–200 nm were thought to be multimicellar aggregates (Fig. 6a–c). In the case of **2B-P2K** without a lipophilic tail, the formation of vesicles (D_a = ∼35 nm) was observed (Fig. 6d).

We next examined the generation of ROS from C_LFC_H complexes under photoirradiation. By monitoring the $^1O_2$-mediated conversion of 9,10-anthracenedipropionic acid (ADPA) to its endoperoxide in UV-vis spectra,[6c,18] we observed that the photoenergy transfer from the excited CFC to oxygen molecules took place in all cases to generate reactive $^1O_2$ efficiently (Fig. 7a). The $^1O_2$ generation efficiency of C_LFC_Hs (Abs/Abs_0 = 0.43–0.56 after photoirradiation for 10 min) is slightly better than that of the reported C_{60}-containing liposomes (Abs/Abs_0 = 0.8 after photoirradiation for 60 min).[6,19]

 © 2022 The Author(s). Published by the Royal Society of Chemistry

Open Access Article. Published on 18 October 2021. Downloaded on 12/9/2025 7:48:21 AM.
This article is licensed under a Creative Commons Attribution-NonCommercial 3.0 Unported Licence.

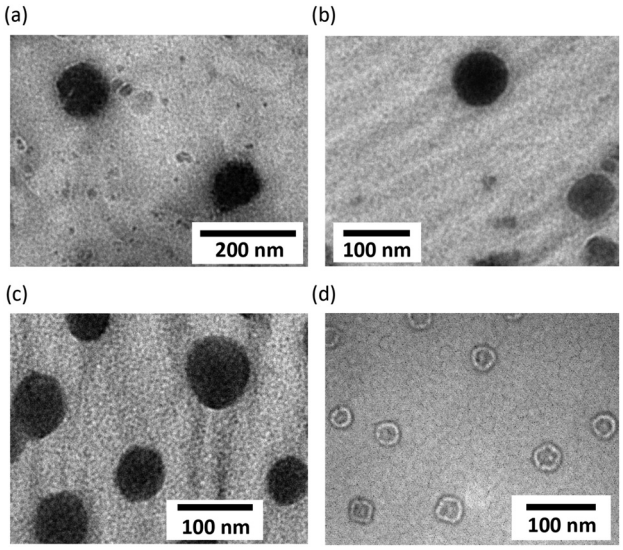

Fig. 6 Selected TEM images of (a) **2A-VE-P5K**, (b) **2A-ICG-P5K**, (c) **2B-VE-P2K** and (d) **2B-P2K**.

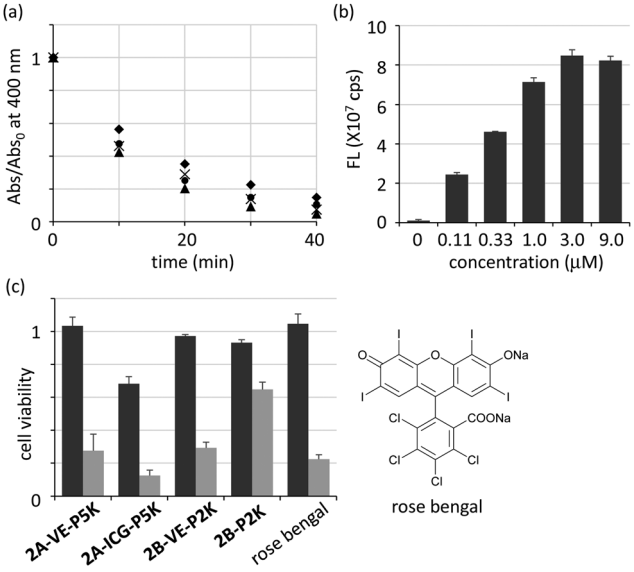

Fig. 7 (a) Time-dependent absorbance (Abs) changes of ADPA at 400 nm with **2A-VE-P2K** (circle), **2A-ICG-P2K** (diamond), **2B-VE-P2K** (triangle) and **2B-P2K** (cross) under photoirradiation (17 mW cm^{-2}, λ = 400–800 nm). Abs_0: Abs of ADPA before irradiation. Abs and Abs_0 are the mean value of two independent experiments. (b) Fluorescence intensities of HeLa cells (1.0×10^3 cells per well) after incubation with **2A-ICG-P5K** for 24 h. Error bars indicate s.d. (n = 3). (c) Cell viability of amphiphilic C_LFC_H complexes and rose bengal (control) after 24 h from the irradiation of visible light (5.1 mW·cm^{-2}, λ = 400–800 nm) for 1 h. Dark grey/pale grey: without/with photoirradiation. Error bars indicate s.d. (n = 3).

From the titration analysis, the effect of $O_2^{\bullet-}$ generation is negligible (Fig. S7 in the ESI†).

The uptake of self-assemblies of **2A-ICG-P5K** by HeLa cells was examined by utilizing near-infrared fluorescence imaging (Fig. 7b and Fig. S8 in the ESI†). After the treatment of HeLa cells with **2A-ICG-P5K** for 24 h, it was confirmed that the fluorescence intensity from HeLa cells was significantly increased as its initial concentration increased. The fluorescence intensities from HeLa cells reached a plateau when its concentration was more than 3 μM, which implies that the intracellular concentration of **2A-ICG-P5K** was saturated after incubation for 24 h. Although the localization of the ICG moiety in the cell membrane may induce fluorescence increment, these results suggest that CFC derivatives have an ability to internalize into living cells.

Finally, we investigated the photoinduced cytotoxicity after 24 h from photoirradiation by using HeLa cells cultured with amphiphilic C_LFC_H complexes in Dulbecco's modified Eagle's medium (Fig. 7c). 75% of cells treated with **2A-VE-P5K** died after photoirradiation, while almost all of the cells survived without photoirradiation. **2A-ICG-P5K** which has a little inherent toxicity also showed photoinduced cytotoxicity. **2B-VE-P2K**, whose structure is similar to **2A-VE-P5K**, exhibits similar photoinduced cytotoxicity, indicating that the photodynamic activity of the contaminated non-capsulated C_{60} is negligible. Vesicles consisting of PEGylated complex **2B-P2K** were photodynamically less active than VE-grafted CFCs in cell experiments, probably because of low cellular uptake of large vesicles. Compared with rose bengal[20] which is one of the most effective photosensitizers in the visible region, the cytotoxicity of **2A-VE-P5K** and **2B-VE-P2K** was comparable under the conditions. By considering the advantage of nanoparticles in passive accumulation,[5] VE-conjugated CFCs with high photodynamic activity will be a valuable candidate as a PDT drug for cancer.

Conclusions

We succeeded in the preparation of amphiphilic γ-CD–C_{60} 2 : 1 complexes, C_LFC_Hs, having both lipophilic and hydrophilic tails by HSVM and sequential filtration. We also demonstrated the alternative synthesis of amphiphilic C_LFC_H through the conventional condensation reaction of CFCs having amino groups with activated esters. We demonstrated that self-assemblies consisting of VE-grafted C_LFC_H complexes showed high photodynamic activity and high photoinduced cytotoxicity. By considering that nanoparticles can accumulate in a tumour site through the enhanced permeability and retention effect,[5] nanoparticles consisting of C_LFC_H complexes are assumed to be one of the promising PDT drugs for malignant cancers. Advanced application in cancer PDT using VE-grafted C_LFC_H having tumour-targeting molecules is underway.

Experimental section

General

The preparation and characterization of functionalized γ-CDs **1** are summarized in the ESI.† The details of the measurement of hydrodynamic diameters, the detection of singlet oxygen and superoxide radical anions under photoirradiation, the cell uptake of **2A-ICG-P2K**, and cytotoxicity evaluation are summarized in the ESI.† UV-vis absorption spectra were recorded using an UV-vis spectrophotometer (V-570, JASCO Co., Japan).

Open Access Article. Published on 18 October 2021. Downloaded on 12/9/2025 7:48:21 AM.
This article is licensed under a Creative Commons Attribution-NonCommercial 3.0 Unported Licence.

Transmission electron microscopy (TEM, JEM-1400, JEOL Ltd, Japan) was used to visualize the morphology of dried self-assemblies. Samples were dropped onto a TEM copper grid covered with a carbon film (200 mesh, Nisshin EM, Japan) and dried for 3 h.

Synthesis of 2A

Throughout the present study, we used an in-house built mill which consisted of a capsule and a milling ball made of stainless steel (Fe–Cr–Ni with a composition of 74 : 18 : 8 by weight). The capsule containing the milling ball was fixed in a vibrating machine so that the capsule could be shaken along its long axis horizontally at a rate of 3500 cycles min^{-1} (rotations per minute (rpm)). Alternatively, HSVM utilizing a commercial apparatus, mixer mill MM400 (Retsch, Germany, 1800 rpm), with a stainless grinding jar and a mixing ball also afforded the corresponding CFCs. UV-vis absorbance measurement suggests that the crude product is a mixture of the C_LFC_H complex (∼20%), the C_HFC_H complex (<10%), and water-insoluble materials containing the C_LFC_L complex and unreacted fullerene (50–60%). The signal of fullerene was not clearly detected in ^{13}C NMR measurement. X-ray photoelectron spectroscopy (XPS) analysis suggested the existence of C═C bonds (Fig. S5 in the ESI†).

A typical procedure is as follows: fullerene C_{60} (2.5 mg, 3.5 μmol), **1-P5K** (22 mg, 3.5 μmol) and **1-ICG** (6.6 mg, 3.5 μmol) were weighed into a stainless capsule together with a mixing ball. The materials were thoroughly mixed by the HSVM technique for 30 min. The mixture was suspended in *ca.* 2 mL water, and the resulting suspension was filtered through a syringe filter (pore size: 0.45 μm, PVDF) to give a clear green solution. After the ultrafiltration of the resulting green solution with a membrane filter (VIVASPIN 20, MWCO: 50 K, PES, Sartorius Stedim Biotech (Germany)), followed by lyophilization of the residue, CFC **2A-ICG-P5K** (5.0 mg, 0.56 μmol, 16% yield, MW(theor) = 8.9 K) was obtained as a green solid. The yield was calculated by using the theoretical molecular weight of C_LFC_H **2A-ICG-P5K**. **2A-ICG-P5K**: IR (KBr) 527, 666, 720, 843, 926, 963, 1009, 1031, 1061, 1109, 1149, 1242, 1281, 1343, 1360, 1421, 1467, 1655, 2886, 3400 cm^{-1}. ^1H NMR (400 MHz, DMSO-d_6, 25 °C) δ 1.30–1.75 (m, 10H), 1.91 (br s, 12H), 3.21–3.62 (overlapped with HDO, m, 11383H), 4.09–4.28 (m, 4H), 4.35–4.55 (m, 48H), 4.86–4.89 (m, 16H), 5.70–5.98 (m, 32H), 6.38–6.42 (m, 2H), 6.52–6.58 (m, 2H), 7.45–7.71 (m, 9H), 7.81–8.27 (m, 8H).

C_LFC_H **2A-VE-P5K** was similarly prepared. **2A-VE-P5K** (a brown solid, 7.7 mg, 0.87 μmol, 25% yield, MW(theor) = 8.8 K): IR (KBr) 527, 709, 760, 744, 942, 1003, 1029, 1084, 1107, 1154, 1252, 1343, 1416, 1458, 1542, 1561, 1655, 2875, 2895, 2926, 3369 cm^{-1}. ^1H NMR (400 MHz, DMSO-d_6, 25 °C) δ 0.82 (br s, 12H), 1.07–1.52 (m, 28H), 1.97 (s, 3H), 2.04 (s, 3H), 2.07 (s, 3H), 3.18–3.62 (overlapped with HDO, m, 1206H), 3.97–4.11 (m, 4H), 4.35–4.60 (m, 24H), 4.38–4.58 (m, 8H), 5.70–6.01 (m, 16H), 7.74 (s, 2H).

Synthesis of 2B-VE-P2K

To a solution of $\mathbf{C_{NH2}FC_{NH2}}$ (16 mg, 3.7 μmol) in water (5 mL) were added **VE-PFP** (12 mg, 19 μmol) in THF (0.5 mL) and **P2K-PFP** (41 mg, 19 μmol) in water (0.5 mL) at room temperature. After stirring for 24 h, the insoluble materials were removed by filtration by using a syringe filter (pore size: 0.45 μm, PVDF). After the ultrafiltration of the resulting brown solution with the membrane filter (VIVASPIN 20, MWCO: 50K, PES, Sartorius Stedim Biotech (Germany)), followed by lyophilization of the residue, C_LFC_H complex **2B-VE-P2K** (3.8 mg, 0.63 μmol, 17% yield, containing ∼10% of the inseparable γ-CD derivative conjugated with P2K) was obtained as a brown solid. IR (ATR) 604, 720, 730, 898, 1207, 989, 1006, 1100, 1027, 1134, 1474, 1520, 1654, 1777, 2850, 2917, 3365 cm^{-1}. ^1H NMsR (400 MHz, DMSO-d_6, 25 °C) δ 0.80–0.89 (m, 12H), 1.05–1.95 (m, 33H), 2.02–2.20 (m, 6H), 2.90–3.90 (overlapped with HDO, m, 15001H), 4.51–4.58 (m, 16H), 4.85–5.01 (m, 16H), 5.75–6.05 (m, 32H), 7.97 (s, 1H). The signal of fullerene was not clearly detected in ^{13}C NMR measurement. XPS analysis suggested the existence of C═C bonds (Fig. S5 in the ESI†).

Synthesis of 2B-P2K

A solution of $\mathbf{C_{NH2}FC_{NH2}}$ (14 mg, 2.1 μmol) and **P2K-PFP** (24 mg, 11 μmol) in water (2 mL) was stirred at room temperature for 24 h. After the ultrafiltration of the reaction mixture with a membrane filter (MWCO: 50K), followed by lyophilization of the residue, CFC **2B-P2K** (4.7 mg, 0.88 μmol, 42% yield, MW(theor) = 5.3 K) was obtained as a pale brown solid. IR (ATR) 578, 843, 940, 1024, 1078, 1106, 1343, 1641, 3338 cm^{-1}. ^1H NMR (400 MHz, D_2O, 25 °C) δ 3.21–3.85 (m, 17169H), 4.44–4.60 (m, 16H), 4.82–4.91 (16H), 5.75–6.05 (m, 32H). The signal of fullerene was not clearly detected in ^{13}C NMR measurement. XPS analysis suggested the existence of C═C bonds (Fig. S5 in the ESI†).

Author contributions

KM, ZDZ, KKa, YK and YM synthesized CFC complexes. KM, ZDZ, KKa, YK, KKo and AE evaluated the optical properties and ROS generation. Cell experiments were conducted by KM, KKa, MO and HH. TEM observation was done by KM and KN. KO directed the project. The manuscript was written by KM and KO. All authors discussed and commented on the manuscript.

Conflicts of interest

There are no conflicts to declare.

Acknowledgements

This work was supported by JSPS KAKENHI Grant Numbers 26708024, 15H00739, 15H00939, and 18H04404, and the Research program for Precursory Research for Embryonic Science and Technology (PRESTO) from Japan Science and Technology Agency (JST), Japan. A part of this study was conducted through the Joint Usage Program of the Radiation Biology Center, Kyoto University. K. M. thanks the Takeda Science Foundation for financial support. We acknowledged Prof. Jun Terao in the University of Tokyo and Assistant Prof. Susumu Tsuda in Osaka Dental University for their support to prepare γ-CD derivatives, and Prof. Teruyuki Kondo and Associate Prof. Yu Kimura in Kyoto University for TEM

 © 2022 The Author(s). Published by the Royal Society of Chemistry

Open Access Article. Published on 18 October 2021. Downloaded on 12/9/2025 7:48:21 AM.
This article is licensed under a Creative Commons Attribution-NonCommercial 3.0 Unported Licence.

measurement. We are indebted to CycloChem Co., Ltd, for generous gifts of γ-CD.

Notes and references

1 (*a*) X. Zhao, J. Liu, J. Fan, H. Chao and X. Peng, *Chem. Soc. Rev.*, 2021, **50**, 4185–4219; (*b*) F. Wei, T. W. Rees, X. Liao, L. Ji and H. Chao, *Coord. Chem. Rev.*, 2021, **432**, 213714; (*c*) P.-C. Lo, M. S. Rodríduez-Morgade, R. K. Pandey, D. K. P. Ng, T. Torres and F. Dumoulin, *Chem. Soc. Rev.*, 2020, **49**, 1041–1056; (*d*) X. Dai, T. Du and K. Han, *ACS Biomater. Sci. Eng.*, 2019, **5**, 6342–6354; (*e*) M. Yang, T. Yang and C. Mao, *Angew. Chem., Int. Ed.*, 2019, **58**, 14066–14080.

2 (*a*) Á. Juarranz, P. Jaén, F. Sanz-Rodríguez, J. Cuevas and S. González, *Clin. Transl. Oncol.*, 2008, **10**, 148–154; (*b*) Y.-Y. Wang, Y.-C. Liu, H. Sun and D.-S. Guo, *Coord. Chem. Rev.*, 2019, **395**, 46–62; (*c*) V.-N. Nguyen, Y. Yan, J. Zhao and J. Yoon, *Acc. Chem. Res.*, 2021, **54**, 207–220.

3 (*a*) M. Wang, Y. Huang, F. F. Sperandio, L. Huang, S. K. Sharma, P. Mroz, M. R. Hamblin, L. Y. Chiang, in *Carbon Nanomaterials for Biomedical Applications*, ed. M. Zhang, R. R. Naik and L. Dai, Springer, Switzerland, 2016, pp. 145–200; (*b*) M. R. Hamblin, *Photochem. Photobiol. Sci.*, 2018, **17**, 1515–1533; (*c*) J. W. Arbogast, A. P. Darmanyan, C. S. Foote, Y. Rubin, F. N. Diederich, M. M. Alvarez, S. J. Anz and R. L. Whetten, *J. Phys. Chem.*, 1991, **95**, 11.

4 (*a*) D. Antoku, K. Sugikawa and A. Ikeda, *Chem. – Eur. J.*, 2019, **25**, 1854–1865; (*b*) T. Eom, V. Barát, A. Khan and M. C. Stuparu, *Chem. Sci.*, 2021, **12**, 4949–4957; (*c*) R. Kawasaki, D. Antoku, R. Ohdake, K. Sugikawa and A. Ikeda, *Nanoscale Adv.*, 2020, **2**, 4395–4399; (*d*) A. Y. Rybkin, A. Y. Belik, O. A. Kraevaya, E. A. Khakina, A. V. Xhilenkov, N. S. Goryachev, D. Volyniuk, J. V. Grazulevicius, P. A. Troshin and A. I. Kotelnikov, *Dyes Pigm.*, 2019, **160**, 457–466; (*e*) A. Narumi, T. Nakazawa, K. Shinohara, H. Kato, Y. Iwaki, H. Okimoto, M. Kikuchi, S. Kawaguchi, S. Hino, A. Ikeda, M. S. A. Shaykoon, X. Shen, Q. Duan, T. Kakuchi, K. Yasuhara, A. Nomoto, Y. Mikata and S. Yano, *Chem. Lett.*, 2019, 1209–1212; (*f*) Y. Zhang, H. Zhang, Q. Zou, R. Xing, T. Jiao and X. Yan, *J. Mater. Chem. B*, 2018, **6**, 7335–7342; (*g*) K. Mizuki, S. Matsumoto, T. Honda, K. Maeda, S. Toyama, D. Iohara, F. Hirayama, S. Okazaki, K. Takeshita and T. Hatta, *Chem. Pharm. Bull.*, 2018, **66**, 822–825.

5 Y. Matsumura and H. Maeda, *Cancer Res.*, 1986, **46**, 6387–6392.

6 (*a*) D. Antoku, S. Satake, T. Mae, K. Sugikawa, H. Funabashi, A. Kuroda and A. Ikeda, *Chem. – Eur. J.*, 2018, **24**, 7335–7339; (*b*) A. Ikeda, T. Mae, M. Ueda, K. Sugikawa, H. Shigeto, H. Funabashi, A. Kuroda and M. Akiyama, *Chem. Commun.*, 2017, **53**, 2966–2969; (*c*) A. Ikeda, T. Iizuka, N. Maekubo, K. Nobusawa, K. Sugikawa, K. Koumoto, T. Suzuki, T. Nagasaki and M. Akiyama, *Chem. Asian J.*, 2017, **12**, 1069–1074; (*d*) A. Ikeda, *Chem. Rec.*, 2016, **16**, 249–260 and references therein.

7 (*a*) T. Andersson, K. Nilsson, M. Sundhal, G. Westman and O. Wennerström, *J. Chem. Soc., Chem. Commun.*, 1992, **28**, 604–606; (*b*) Z.-i. Yoshida, H. Takekuma, S.-i. Takekuma and Y. Matsubara, *Angew. Chem., Int. Ed. Engl.*, 1994, **33**, 1597–1599.

8 (*a*) X. Zhu, S. Xiao, D. Zhou, M. Sollogoub and Y. Zhang, *Eur. J. Med. Chem.*, 2018, **146**, 194–205; (*b*) X. Zhu, A. Quaranta, R. V. Bensasson, M. Sollogoub and Y. Zhang, *Chem. – Eur. J.*, 2017, **23**, 9462–9466; (*c*) K. Nobusawa, D. Payra and M. Naito, *Chem. Commun.*, 2014, **50**, 8339–8342; (*d*) Y. Takeda, T. Nagamachi, K. Nishikori and S. Minakata, *Asian J. Org. Chem.*, 2013, **2**, 69–73; (*e*) H. M. Wang and G. Wenz, *Beilstein J. Org. Chem.*, 2012, **8**, 1644–1651; (*f*) C. O. Mellet, J. M. Benito and J. M. G. Fernández, *Chem. – Eur. J.*, 2010, **16**, 6728–6742.

9 (*a*) K. Komatsu, *Top. Curr. Chem.*, 2005, **254**, 185–206; (*b*) S.-E. Zhu, F. Li and G.-W. Wang, *Chem. Soc. Rev.*, 2013, **42**, 7535–7570; (*c*) G.-W. Wang, *Chin. J. Chem.*, 2021, **39**, 1797–1803.

10 K. Komatsu, K. Fujiwara, Y. Murata and T. Braun, *J. Chem. Soc., Perkin Trans. 1*, 1999, 2963–2966.

11 (*a*) J. F. R. Van Guyse, V. R. de la Rosa, R. Lund, M. De Bruyne, R. De Rycke, S. K. Filippov and R. Hoogenboom, *ACS Macro Lett.*, 2019, **8**, 172–176; (*b*) J. F. R. Van Guyse, V. R. de la Rosa and R. Hoogenboom, *Chem. – Eur. J.*, 2018, **24**, 2758–2766.

12 W. Tang and S.-C. Ng, *Nat. Protoc.*, 2008, **3**, 691–697.

13 B. E. Schaafsma, J. S. D. Mieog, M. Hutteman, J. R. van der Vorst, P. J. K. Kuppen, C. W. G. M. Löwik, J. V. Frangioni, C. J. H. van de Velde and A. L. Vahrmeijer, *J. Surg. Oncol.*, 2011, **104**, 323–332.

14 Although C_LFC_Hs were supposed to be a mixture of diastereoisomers related to the position of lipophilic and hydrophilic tails, they could not be assigned by variable-temperature ^1H NMR in D_2O.

15 Because fullerene derivatives and γ-CD can form a water-soluble aggregate, the production of this aggregate could not be excluded. (*a*) H. Jiao, S. H. Goh and S. Valiyaveettil, *Macromolecules*, 2002, **35**, 1399–1402; (*b*) D. Iohara, F. Hirayama, K. Higashi, K. Yamamoto and K. Uekama, *Mol. Pharm.*, 2011, **8**, 1276–1284; (*c*) D. Iohara, F. Hirayama, M. Anraku and K. Uekama, *ACS Appl. Nano Mater.*, 2019, **2**, 716–725.

16 (*a*) K. Takechi, P. K. Sudeep and P. V. Kamat, *J. Phys. Chem. B*, 2006, **110**, 16169–16173; (*b*) F. Rotermund, R. Weigand and A. Penzkofer, *Chem. Phys.*, 1997, **220**, 385–392.

17 Because ICG is known to be decomposed by photoirradiation under air, the absorbance of **2A-ICG-P5K** was gradually decreased under visible light and oxygen atmosphere. W. Holzer, M. Mauerer, A. Penzkofer, R.-M. Szeimies, C. Abels, M. Landthaler and W. Bäumler, *J. Photochem. Photobiol., B*, 1998, **47**, 155–164.

18 B. A. Lindig, M. A. J. Rodgers and A. P. Schaap, *J. Am. Chem. Soc.*, 1980, **102**, 5590–5593.

19 (*a*) A. Ikeda, M. Akiyama, T. Ogawa and T. Takeya, *ACS Med. Chem. Lett.*, 2010, **1**, 115–119; (*b*) A. Ikeda, T. Iizuka, N. Maekubo, R. Aono, J.-I. Kikuchi, M. Akiyama, T. Konishi, T. Ogawa, N. Ishida-Kitagawa, H. Tatebe and K. Shiozaki, *ACS Med. Chem. Lett.*, 2013, **4**, 752–756.

20 (*a*) R. W. Redmond and J. N. Gamlin, *Photochem. Photobiol.*, 1999, **70**, 391–475; (*b*) E. Gandin, Y. Lion and A. van de Vorst, *Photochem. Photobiol.*, 1983, **37**, 271–278.